

# Abrupt climate change and collapse of deep-sea ecosystems

Moriaki Yasuhara\*<sup>†‡</sup>, Thomas M. Cronin\*, Peter B. deMenocal<sup>§</sup>, Hisayo Okahashi\*<sup>†</sup>, and Braddock K. Linsley<sup>¶</sup>

\*U.S. Geological Survey, 926A National Center, Reston, VA 20192; <sup>§</sup>Lamont-Doherty Earth Observatory of Columbia University, Palisades, NY 10964; and <sup>¶</sup>Department of Earth and Atmospheric Sciences, University at Albany, State University of New York, Albany, NY 12222

Edited by James P. Kennett, University of California, Santa Barbara, CA, and approved December 12, 2007 (received for review June 13, 2007)

**We investigated the deep-sea fossil record of benthic ostracodes during periods of rapid climate and oceanographic change over the past 20,000 years in a core from intermediate depth in the northwestern Atlantic. Results show that deep-sea benthic community “collapses” occur with faunal turnover of up to 50% during major climatically driven oceanographic changes. Species diversity as measured by the Shannon–Wiener index falls from 3 to as low as 1.6 during these events. Major disruptions in the benthic communities commenced with Heinrich Event 1, the Inter-Allerød Cold Period (IACP: 13.1 ka), the Younger Dryas (YD: 12.9–11.5 ka), and several Holocene Bond events when changes in deep-water circulation occurred. The largest collapse is associated with the YD/IACP and is characterized by an abrupt two-step decrease in both the upper North Atlantic Deep Water assemblage and species diversity at 13.1 ka and at 12.2 ka. The ostracode fauna at this site did not fully recover until 8 ka, with the establishment of Labrador Sea Water ventilation. Ecologically opportunistic slope species prospered during this community collapse. Other abrupt community collapses during the past 20 ka generally correspond to millennial climate events. These results indicate that deep-sea ecosystems are not immune to the effects of rapid climate changes occurring over centuries or less.**

deglacial–Holocene Ostracoda species diversity macroecology paleoceanography

There is growing evidence that deep-sea benthic ecosystems are variable in structure and diversity over various spatial and temporal scales (e.g., local, regional, global, seasonal, millennial, orbital) (1–3), modifying the long-held view of stability embodied in the stability–time hypothesis (4, 5). Climatic and oceanographic changes must be considered important factors influencing deep-sea ecosystems. Whereas the sensitivity of terrestrial, oceanic surface, and shallow marine ecosystems to historical climate change has been established (6–8), little is known about the impact of rapidly changing climate on deep-sea ecosystems (9). The availability of sediment cores from regions of the ocean characterized by high sedimentation and well preserved fossil Ostracoda offers an opportunity to examine the sensitivity of deep-sea organisms to well known abrupt climate events of the past 20,000 years including the current Holocene interglacial period.

Ostracodes are small bivalved Crustacea that form an important component of deep-sea meiobenthic communities along with nematodes and copepods (10). Crustaceans, including Ostracoda, Decapoda, Isopoda, Cumacea, Copepoda, and Amphipoda, are dense and diverse in the deep sea and one of the most representative groups of whole deep-sea benthic community (10, 11). Ostracode species have a variety of habitat and ecology preferences (e.g., infaunal, epifaunal, scavenging, and detrital feeders) (12–14), representing a wide range of deep-sea soft sediment niches. Furthermore, Ostracoda is the only commonly fossilized metazoan group in deep-sea sediments. Thus, fossil ostracodes are considered to be generally representative of the broader benthic community. The distribution and abundance of deep-sea ostracode taxa in the North Atlantic Ocean are

influenced by several factors, among them, temperature, oxygen, sediment flux, and food supply (14, 15). Several paleoecological studies suggest that these factors influence deep-sea ecosystems over orbital and millennial timescales (1, 16).

Ocean Drilling Program (ODP) Hole 1055B was cored at the Carolina Slope in the western subtropical North Atlantic (32°47.041 N, 76°17.179 W; 1,798 m water depth) during ODP Leg 172 (17). Sediment accumulation rates in this sediment drift average 23 cm per thousand years (kyr). This site is sensitive to changes in deep-water circulation because it is within the basal core of Upper North Atlantic Deep Water (UNADW) composed of Labrador Sea Water (LSW) (17). Surface-water temperature and productivity are also variable in this region, which is located in the path of the Gulf Stream (18).

Here we report a detailed 20-kyr record of deep-sea benthic ostracodes from ODP site 1055 and compare ostracode community and diversity variability to abrupt paleoclimate and oceanographic events over this interval. Results show that deep-sea benthic communities frequently experience “community collapses” coincident with large, abrupt changes in deep-ocean circulation and climate.

## Results and Discussion

The ODP 1055 high-resolution ostracode relative abundance record demonstrates that the deglacial–Holocene deep-sea community was highly unstable, characterized by many large (up to 50%) centennial–millennial scale turnovers in faunal composition (Fig. 1). Assemblage structure and diversity are clearly disturbed during centennial–millennial scale cooling events recognized in the last deglacial and Holocene intervals in the Greenland ice core (GISP2) (19–21) and North Atlantic deep-sea sediment core (22, 23) records (Fig. 2; see below). These include Holocene cooling events (HCE) 0–8 defined by Bond *et al.* (22, 23), the Younger Dryas (YD), the Inter-Allerød Cold Period (IACP), and Heinrich Event 1 (H1). A number of paleoceanographic studies have demonstrated dramatic and abrupt deep-water circulation changes during these cooling events (22, 24–27) (Fig. 2).

The ostracode relative abundance and species diversity calculations and CABFAC factor analysis are based on three-point moving sums of the census dataset. Calculations based on raw census datasets are more variable and, in the case of species diversity  $H(S)$ , slightly underestimated because of relatively

Author contributions: M.Y. and T.M.C. designed research; M.Y., P.B.d.M., H.O., and B.K.L. performed research; M.Y., P.B.d.M., and B.K.L. analyzed data; and M.Y. and T.M.C. wrote the paper.

The authors declare no conflict of interest.

This article is a PNAS Direct Submission.

<sup>†</sup>Present address: Department of Paleobiology, National Museum of Natural History, Smithsonian Institution, Washington, DC 20013-7012.

<sup>‡</sup>To whom correspondence should be addressed: E-mail: moriakiyasuhara@gmail.com or yasuharam@si.edu.

This article contains supporting information online at [www.pnas.org/cgi/content/full/0705486105/DC1](http://www.pnas.org/cgi/content/full/0705486105/DC1).

© 2008 by The National Academy of Sciences of the USA

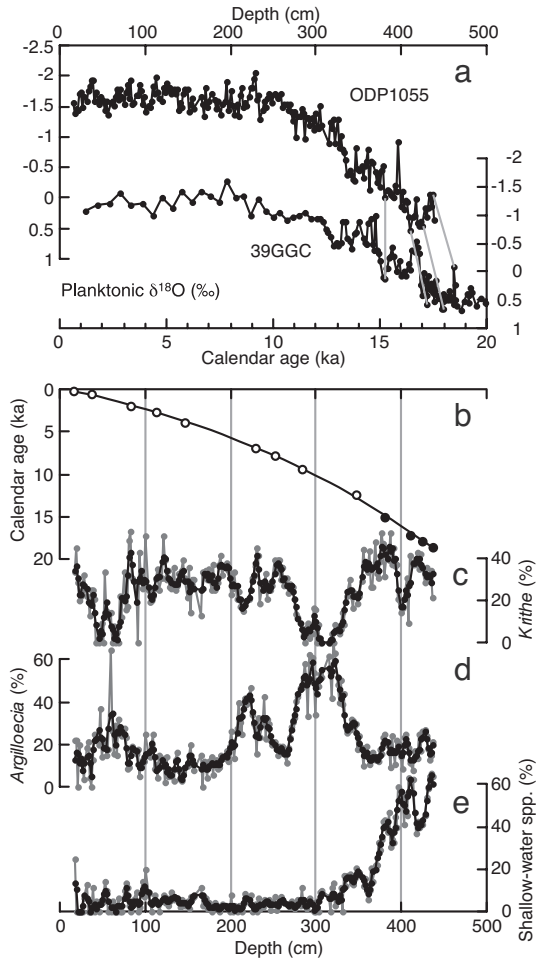


**Fig. 1.** Chronology and ostracode relative abundance data from ODP site 1055. (a) The planktonic foraminifera  $\delta^{18}\text{O}$  and its correlation to the well dated record of nearby core 39GGC (gray lines; SI Table 3). (b) Age model (open circles, AMS radiocarbon dates; filled circles,  $\delta^{18}\text{O}$  correlation-based age-control points). (c and d) Relative abundance of two dominant ostracode genera *Krithe* and *Argilloecia*. (e) Percentage of shallow-water taxa in total ostracodes. Gray plots, calculations based on raw ostracode census dataset; black plots, calculations based on three-point moving sum census dataset.

small sample size (70 specimens per sample on average), but quite similar to results based on three-point moving sum census datasets (Figs. 1–3).

As a result of Q mode CABFAC factor analysis, two varimax factors were calculated, which represent 89.6% of the total variance. The first factor accounts for 57.3% of the total variance and is characterized by high varimax scores for *Krithe* (0.903) and *Cytheropteron* (0.295). *Krithe* is a typical deep-water genus and an especially important component of NADW fauna (28). *Cytheropteron* is predominant in NADW in the North Atlantic (12). The second factor, representing 32.3% of the total variance, is characterized by the high varimax score of *Argilloecia* (0.966). This genus was the most common taxon living in the oxygen minimum zone of the upper continental slope off southeastern North America (29). *Argilloecia* is also an important component of late Pleistocene (16) and Pliocene (30) faunas from the Mid-Atlantic Ridge that represent climatic transitions, especially deglacial periods and interstadial-stadial transitions. Its predominance in modern low-oxygen, often organic rich bottom sediments and during climatic transitions suggests an opportunistic ecology. Other genera (*Henryhowella* and *Cytherella*) having relatively high varimax scores (0.123 and 0.127, respectively)

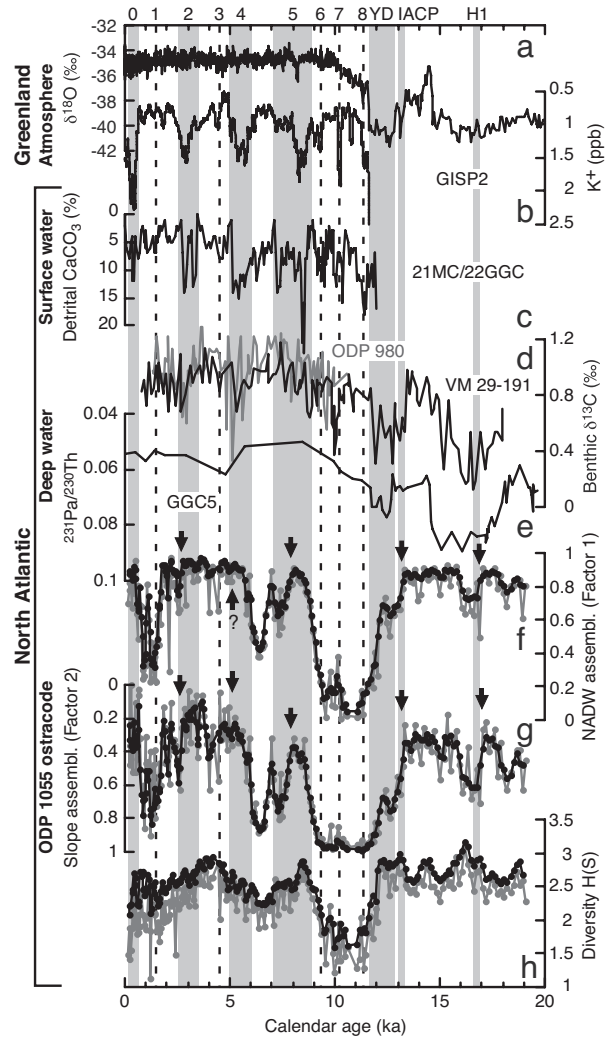


**Fig. 2.** Deglacial to Holocene variations in ostracode faunal assemblages from ODP site 1055 compared with proxy records of Greenland atmosphere and North Atlantic surface and deep water. (a and b) The Greenland ice core GISP2  $\delta^{18}\text{O}$  proxy for temperature (a) and potassium (K : 60-point moving average) ion proxy for the Siberian High (19–21, 72) (b). (c) Northwestern Atlantic core KNR158-4-21MC/22GGC percent detrital  $\text{CaCO}_3$  proxy for ice rafted debris events (23). (d and e) Northeastern Atlantic cores VM29-191 (black) and ODP 980 (gray) benthic foraminifera  $\delta^{13}\text{C}$  (22, 26) (d) and northwestern Atlantic core OCE326-GGC5 sedimentary  $^{231}\text{Pa}/^{230}\text{Th}$  (232-based) (27) proxies for the deep-water circulation (e). (f and g) The varimax factor loadings of the first and second factors interpreted as UNADW and slope assemblages, respectively. (h) Ostracode species diversity shown as Shannon-Wiener index, H(S). Bond's HCE 0–8, YD, IACP, and H1 are indicated by shading (major events) and dashed line (smaller events). The HCE 0 is equivalent to the Little Ice Age. Arrows show inceptions of oyster events. Gray plots, calculations based on raw ostracode census dataset; black plots, calculations based on three-point moving sum census dataset.

also inhabit slope water (29, 31). Thus, we interpret factor 1 as an UNADW assemblage typical of the Carolina Slope region where modern UNADW and Glacial North Atlantic Intermediate Water (GNAIW) originating in the Labrador Sea region predominate. Factor 2 is a slope assemblage comprising opportunistic species typical of continental margin habitats.

The distribution of modern deep-sea ostracode assemblages is not solely controlled by deep-water properties, but other factors such as surface primary production, the main food source for many deep-sea organisms (32–35), can also affect the benthic assemblage composition. Nonetheless, recent ecological re-

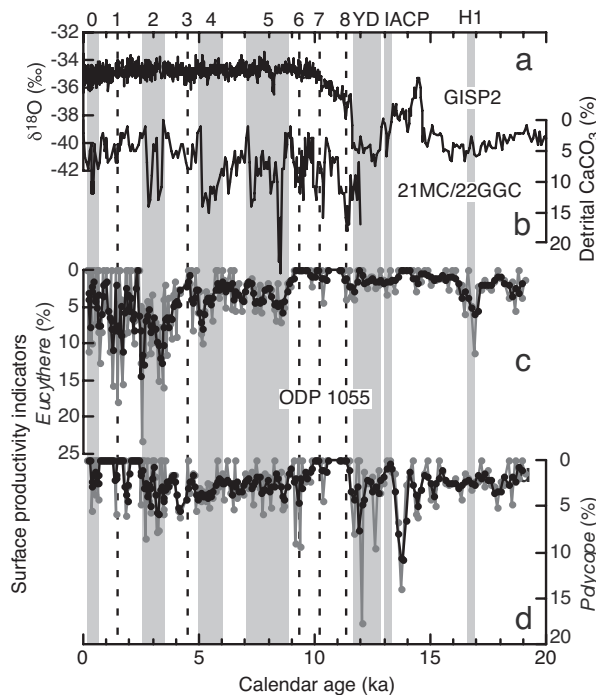


**Fig. 3.** Deglacial to Holocene variations in ostracodes from ODP site 1055 indicative of surface productivity, compared with proxy records for atmosphere and surface-water changes in North Atlantic region. GISP2  $\delta^{18}\text{O}$  (19) (a), KNR158-4-21MC/22GGC percent detrital  $\text{CaCO}_3$  (23) (b), and ODP 1055 *Eucythere* (c), and *Polycope* relative abundance (d). Gray plots, calculations based on raw ostracode census dataset black plots, calculations based on three-point moving sum census dataset.

search suggests that metazoan meiobenthos may be less sensitive to changes in surface productivity than protozoan Foraminifera (36). Furthermore, the ostracode genera *Eucythere* and *Polycope*, which are sensitive to changes in surface productivity (14, 37), show a trend different from factor 1, as discussed later, and have only low varimax scores (0.121 and 0.069) for factor 1. Planktonic foraminifera  $\delta^{18}\text{O}$  (Fig. 1) and Mg/Ca ratios (P.B.d.M., unpublished data), which are proxies for surface salinity and temperature, of ODP site 1055 also show a trend different from factor 1. Above-mentioned evidence suggests that our interpretation for factor 1 is reasonable as the first approximation.

Factor 1 (UNADW assemblage) starts to decrease abruptly during all major cooling events: HCE2, HCE4, HCE5, YD, IACP, and H1. Ostracode species diversity H(S) shows similar oscillations, except there are clear decreases only in the YD and HSE5. Conversely, factor 2 (slope assemblage) rapidly increased at these times. The onsets of ostracode faunal events are dated at 2.8, 5.2, 8.0, 13.1, and 17.1 ka, respectively (arrows in Fig. 2); the first two fall within HCE2 and HCE4, respectively. The former ostracode event (HCE2) has several steps that possibly reflect minor cooling events such as HCE1, and the latter ostracode event (HCE4) is not well defined in the UNADW assemblage. The ostracode event beginning near 8.0 ka (HCE5) is characterized by a two-step decrease in the UNADW assemblage and an increase in slope assemblages. The ostracode event beginning 13.1 ka (IACP and continuing through the YD) also has a two-step pattern with marked faunal changes at 13.1 and 12.2 ka. During this event species diversity H(S) dropped from near 3 to 1.6. Each step of faunal changes occurs over 10–30 cm of core, or within a few centuries to 1,000 years. The deep-water community may have even been affected during the most recent Holocene cooling event, the Little Ice Age (38),

equivalent to HCE0, but additional records are needed to confirm this (Fig. 2).

Abrupt centennial and millennial climate events are complex and their causes are not fully understood (39–42). Even less is known about the biotic response to abrupt climate events. Furthermore, LSW, the source water for the core site, is highly unstable even over decadal timescales (43), and longer-term variability of deep-water masses at intermediate (2,000 m) depths after the Last Glacial Maximum (LGM: 26–21 ka) are also complex (44–48). Bioturbation may also complicate the meiofaunal record from sediment cores.

Nonetheless, we propose several viable mechanisms to explain the reconstructed patterns. One apparently enigmatic feature of this record is the similarity between late Holocene and glacial when the UNADW assemblage is dominant during both periods at ODP site 1055 (Fig. 2). However, this should not be surprising because during the last glacial, GNAIW, the glacial analog of modern UNADW, dominated the core site region. Holocene and glacial  $\delta^{13}\text{C}$  values of benthic foraminifera are similar, or even slightly higher for the glacial at intermediate depths (2,000 m) of the northeastern and northwestern Atlantic including almost exactly same site as ODP site 1055, suggesting this site is in the path of vigorous low-nutrient GNAIW during the last glacial period (18, 49).

The relationship between ostracode faunal assemblages and deep-water changes before 15 ka includes relatively small changes in factor loadings and diversity (Fig. 2). For example, the relatively minor ostracode faunal response at H1 event at 16.8 ka (22, 50) may indicate that the magnitude of GNAIW variability was small at intermediate depths (2,000 m). Benthic  $\delta^{13}\text{C}$  data for ODP site 982, northeastern Atlantic, support the view that the magnitude of GNAIW change was smaller during glacial, including Heinrich events, than in deglacial terminations (49).

Alternatively, the interval 17–14.5 ka, which has been called the “mystery interval,” was a time characterized by warm summers and cold winters in the region around the North Atlantic (51). An unusually strong seasonality could affect surface productivity and the resulting food supply to deep-sea benthos. This may mean that the deep-sea community response may not be directly comparable before and after 15 ka. The large proportion of transported shallow-water species during this interval (Fig. 1), a reflection of lower global sea level and proximity of the core site to the paleoshoreline, may also influence the faunal patterns, even though these shallow-water contaminated taxa were excluded from our analyses.

The most significant feature of this ostracode record is the collapse of UNADW assemblages that began with YD/IACP, accompanied by a sharp and large-amplitude species diversity decline (Fig. 2). GNAIW was likely greatly diminished at this time. Deglacial reduction of GNAIW has been well established (45, 49, 52, 53), although its precise timing is less certain because of the absence of high-resolution records. Following this ostracode faunal collapse, the community did not fully recover until

8 ka, which postdates the end of the YD climate reversal. This late recovery is most likely because LSW, constituting UNADW near this site, had not been established until early Holocene, 8 ka (54). During this period, Southern Source Water may have been predominant at intermediate depth on the Carolina Slope as suggested from low-resolution records (45, 49). It should be noted that the actual ocean ventilation during the last deglaciation at intermediate depths is not well known. Available planktonic and benthic foraminiferal  $^{14}\text{C}$  data from the 2,000 m Carolina Slope did not show significant ventilation differences between the beginning of the YD (12.9 ka) and today, suggesting little or no GNAIW reduction at this time (18). This interval corresponds to the very beginning of the ostracode faunal collapse. This is not necessarily inconsistent with our

interpretation of environmental change at this time, but additional, well dated proxy records are needed to resolve the exact timing of GNAIW reduction.

The resulting deep-water environment may have adversely impacted not only the UNADW assemblage, but also the deep-sea community in general, as indicated by low species diversity, which suggests stressed environments. Temperature and/or deep-water current velocity-induced substrate changes may have been important factors controlling deep-sea species diversity (55–57). As a result, the opportunistic slope assemblage may have been able to migrate to this deeper location and temporarily prosper. Such water-mass property change may have caused active downslope and upslope migration of species similar to patterns observed during climate cycles occurring over orbital timescales of 41 kyr and 100 kyr (16, 30) and during the last deglaciation (58).

A similar mechanism may hold for other UNADW assemblage collapses during the Holocene. Although UNADW assemblage started to decrease abruptly during Holocene cooling events, the collapses did not recover within cooling events themselves, possibly because of delayed renewal of LSW. Millennial scale weakening of LSW is also suggested by Hillaire-Marcel *et al.* (54), although the low time resolution of their record does not allow direct comparison.

To confirm the above-mentioned scenario, high-resolution deep-water proxy records (e.g., benthic  $\delta^{13}\text{C}$ ,  $^{231}\text{Pa}/^{230}\text{Th}$ , grain size, etc.) from the 2,000 m depth, that is, the basal core of interglacial LSW and glacial GNAIW, are needed. Currently, all high-resolution records covering the last deglaciation are available from 2,000 m depth, located in the path of lower NADW during interglacials and deglacials and Antarctic Bottom Water (AABW) during glacials. Furthermore, recent studies suggest the possible existence of two sources of GNAIW: one in the south Labrador Sea and another west of Rockall Plateau (59), suggesting possible different behavior of GNAIW between the northeastern and northwestern Atlantic.

In addition to deep-water mass changes, climate change can also affect deep-sea communities in the form of changes in surface primary production of food source for benthic species (32–35). The ostracodes *Eucythere* and *Polycope* are indicators of seasonal and increased surface productivity, respectively (14, 37) (see Fig. 3). These taxa, especially *Eucythere*, show trends similar to those in detrital carbonate in northwestern Atlantic core KNR158-4-21MC/22GGC off Newfoundland (23) since 9 ka, reflecting surface-water changes in the northwestern Atlantic region (Fig. 3). Notably, double spikes during HCE 2 and 5 and the gradual increase and rapid decrease of the relative abundance in the HCE4 characterize both the detrital carbonate and *Eucythere* records. *Polycope* peaks during 15–10 ka correlate closely with peaks in benthic foraminiferal abundance (*Cibicides* spp. and *Uvigerina peregrina*) known from the same region, which is interpreted to represent stronger winter mixing and a more productive surface ocean (18, 60). The differences in these two productivity indicators may reflect different modes of surface productivity during deglacial and Holocene interglacial periods or ecological differences between the two ostracode taxa. Regardless of the precise mechanism, these ostracodes seem to respond to surface productivity changes.

We conclude that at this site the deep-sea ecosystem is highly sensitive to millennial-scale disturbances in habitat driven by climate changes during the deglacial and Holocene intervals. Deglacial and Holocene cooling events have triggered rapid collapses of deep-water benthic communities. Certain groups

sensitive to surface productivity respond immediately to climate-driven oceanographic changes. Our results have bearing on possible long-term effects of human-induced oceanographic changes now in evidence in many instrumental records and biological indicators.

## Materials and Methods

Core 1H from Hole 1055B was continuously sampled at 2-cm intervals, yielding an average sampling resolution of 50–100 years. The 150- $\mu\text{m}$ -size fraction was examined for ostracode faunal composition and diversity. More than 122 species were identified in total. We used the Shannon–Wiener index

$$H S = - \sum_{i=1}^S p_i \ln p_i$$

where  $p_i$  is the proportion of the  $i$ th species,  $\ln$  is the natural log, and  $S$  is the total number of species] for species diversity because it is more widely used than other diversity measures and relatively insensitive to sample size (61). Other representative diversity measures show similar trends [Supporting Information (SI) Fig. 4]. Q-mode CABFAC factor analysis (62) was performed to determine dominant faunal assemblages and their temporal downcore patterns by using 31 ostracode genera occurring as more than three specimens in any sample (Fig. 2 and SI Table 1).

Age control was established with nine accelerator mass spectrometer (AMS) radiocarbon dates and additional four age-control points for the glacial sediments are based on correlation of the oxygen isotope ( $\delta^{18}\text{O}$ ) record to a nearby deeper core, 39GGC (60) (Fig. 1 and SI Tables 2 and 3). The radiocarbon dating and  $\delta^{18}\text{O}$  measurements were performed on planktonic foraminifera *Globigerinoides ruber* (255–300  $\mu\text{m}$ ). Radiocarbon ages were converted to calibrated calendar ages by using CALIB 5.0 (63, 64) based on the Marine04 dataset (65) and a local  $R$  of 65  $\pm$  32 years (66). The core 39GGC was used for the  $\delta^{18}\text{O}$  correlation because it has the highest resolution and sedimentation rate and excellent chronology, especially for the glacial sediments in this region. Furthermore, our ostracode data and Keigwin's study of core 51GGC from almost the same site as ODP 1055 (18) indicate downslope reworking for the glacial sediments of this site, and the deeper site 39GGC was much less influenced by downslope reworking for the sand-size (i.e., foraminifera size) fraction (60). The correlation is based on obvious  $\delta^{18}\text{O}$  features that are common to many detailed  $\delta^{18}\text{O}$  series from this region. The ages for the tie points fit with a third-order polynomial.

Shallow-water taxa transported by downslope processes are relatively minor (< 20% of the total assemblage) for the last 13 kyr and determined mainly based on faunal studies on the shelf (Fig. 1) (67–71). These taxa are excluded from the analyses, that is, from the relative abundance and diversity index calculations and CABFAC factor analysis. Calculated species diversity values may be slightly underestimated because *Argilloecia* and *Polycope* species are lumped (the taxonomy of these genera is not established enough and there are only a few species of these genera per sample).

Carbonate dissolution is not likely to be an influence on ostracode assemblages, because the ostracode valves and carapaces are well preserved and site ODP 1055 is shallower than calcite lysocline and isolated from the influence of potentially corrosive Antarctic Bottom Water (AABW).

Data are available at the National Oceanic and Atmospheric Administration World Data Center for Paleoclimatology, [www.ngdc.noaa.gov/paleo/paleo.html](http://www.ngdc.noaa.gov/paleo/paleo.html).

**ACKNOWLEDGMENTS.** We thank the staff of the U.S. Geological Survey Eastern Earth Surface Processes Team for their support throughout this project, Jerry F. McManus for GGC5 data, Paul A. Mayewski for GISP2 data, Harry J. Dowsett and Debra A. Willard for valuable comments, and Lloyd D. Keigwin and an anonymous referee for constructively critical reviews. This research used samples provided by the Ocean Drilling Program. The Ocean Drilling Program is sponsored by the National Science Foundation and participating countries under the management of Joint Oceanographic Institutions. This work was supported by Japan Society for the Promotion of Science Postdoctoral Fellowships for Research Abroad and Smithsonian Postdoctoral Fellowship (to M.Y.).

1. Cronin TM, Raymo ME (1997) *Nature* 385:624–627.

2. Rex MA, Stuart CT, Coyne G (2000) *Proc Natl Acad Sci USA* 97:4082–4085.

3. Stuart CT, Rex MA, Etter RJ (2003) in *Ecosystems of the Deep Oceans*, ed Tyler PA (Elsevier, Amsterdam), pp 295–311.

4. Hessler RR, Sanders HL (1967) *Deep-Sea Res* 14:65–78.

5. Sanders HL (1968) *Am Nat* 102:243–282.

6. Stenseth NC, Mysterud A, Ottersen G, Hurrell JW, Chan K-S, Lima M (2002) *Science* 297:1292–1296.

7. Walther G-R, Post E, Convey P, Menzel A, Parmesan C, Beebee TJC, Fromentin J-M, Hoegh-Guldberg O, Bairlein F (2002) *Nature* 416:389–395.
8. Parmesan C, Yohe G (2003) *Nature* 421:37–42.
9. Danovaro R, Dell'Anno A, Fabiano M, Pusceddu A, Tselepidis A (2001) *Trends Ecol Evol* 16:505–510.
10. Brandt A, Gooday AJ, Brandão SN, Brix S, Brökeland W, Cédhagen T, Choudhury M, Cornelius N, Danis B, De Mesel I, et al. (2007) *Nature* 447:307–311.
11. Sanders HL, Hessler RR, Hampson GR (1965) *Deep-Sea Res* 12:845–867.
12. Didié C, Bauch HA (2000) *Mar Micropaleontol* 40:105–129.
13. Didié C, Bauch HA (2002) in *The Ostracoda: Applications in Quaternary Research*, eds Holmes JA, Chivas AR (American Geophysical Union, Washington, DC), pp 279–299.
14. Didié C, Bauch HA, Helmke JP (2002) *Palaeogeogr Palaeoclimatol Palaeoecol* 184:195–212.
15. Cronin TM, Boomer I, Dwyer GS, Rodriguez-Lazaro J (2002) in *The Ostracoda: Applications in Quaternary Research*, eds Holmes JA, Chivas AR (American Geophysical Union, Washington, DC), pp 99–119.
16. Cronin TM, DeMartino DM, Dwyer GS, Rodriguez-Lazaro J (1999) *Mar Micropaleontol* 37:231–249.
17. Keigwin LD, Rio D, Acton GD, Bianchi GG, Borowski W, Çagatay N, Chaisson WP, Clement BM, Cortijo E, Dunbar GB, et al. (1998) *Proceedings of the Ocean Drilling Program, Initial Reports* (Ocean Drilling Program, College Station, TX), Vol 172.
18. Keigwin LD (November 18, 2004) *Paleoceanography*, 10.1029/2004PA001029.
19. Grootes PM, Stuiver M, White JWC, Johnsen SJ, Jouzel J (1993) *Nature* 366:552–554.
20. O'Brien SR, Mayewski PA, Meeker LD, Meese DA, Twickler MS, Whitlow SI (1995) *Science* 270:1962–1964.
21. Mayewski PA, Meeker LD, Twickler MS, Whitlow S, Yang Q, Lyons WB, Prentice M (1997) *J Geophys Res* 102:26345–26366.
22. Bond G, Showers W, Cheseby M, Lotti R, Almasi P, deMenocal P, Priore P, Cullen H, Hajdas I, Bonani G (1997) *Science* 278:1257–1266.
23. Bond G, Kromer B, Beer J, Muscheler R, Evans MN, Showers W, Hoffmann S, Lotti-Bond R, Hajdas I, Bonani G (2001) *Science* 294:2130–2136.
24. Bianchi GG, McCave IN (1999) *Nature* 397:515–517.
25. Marchitto TM, deMenocal PB (December 6, 2003) *Geochem Geophys Geosyst*, 10.1029/2003GC000598.
26. Oppo DW, McManus JF, Cullen JL (2003) *Nature* 422:277–278.
27. McManus JF, Francois R, Gherardi J-M, Keigwin LD, Brown-Leger S (2004) *Nature* 428:834–837.
28. Dingle RV, Lord AR (1990) *Palaeogeogr Palaeoclimatol Palaeoecol* 80:213–235.
29. Cronin TM (1983) *Mar Micropaleontol* 8:89–119.
30. Cronin TM, Raymo ME, Kyle KP (1996) *Geology* 24:695–698.
31. Dingle RV, Lord AR, Boomer ID (1990) *Ann S Afr Mus* 99:245–366.
32. Gooday AJ (1988) *Nature* 332:70–73.
33. Thomas E, Booth L, Maslin M, Shackleton NJ (1995) *Paleoceanography* 10:545–562.
34. Thomas E, Gooday AJ (1996) *Geology* 24:355–358.
35. Wollenburg JE, Mackensen A, Kuhnt W (2007) *Palaeogeogr Palaeoclimatol Palaeoecol* 255:195–222.
36. Shimanaga M, Kitazato H, Shirayama Y (2004) *Mar Biol* 144:1097–1110.
37. Cronin TM, Holtz TR, Jr, Stein R, Spielhagen R, Fütterer D, Wollenburg J (1995) *Paleoceanography* 10:259–281.
38. Keigwin LD (1996) *Science* 274:1504–1508.
39. Hughen KA, Southon JR, Lehman SJ, Overpeck JT (2000) *Science* 290:1951–1954.
40. Mayewski PA, Rohling EE, Stager JC, Karlén W, Maasch KA, Meeker LD, Meyerson EA, Gasse F, van Krevelend S, Holmgren K, et al. (2004) *Quat Res* 62:243–255.
41. Denton GH, Alley RB, Comer GC, Broecker WS (2005) *Quat Sci Rev* 24:1159–1182.
42. Stanford JD, Rohling EJ, Hunter SE, Roberts AP, Rasmussen SO, Bard E, McManus J, Fairbanks RG (December 9, 2006) *Paleoceanography*, 10.1029/2006PA001340.
43. Yashayaev I, Bersch M, van Aken HM (May 17, 2007) *Geochem Geophys Geosyst*, 10.1029/2006GL028999.
44. Adkins JF, Cheng H, Boyle EA, Druffel ERM, Edwards RL (1998) *Science* 280:725–728.
45. Hall JM, Chan L-H (December 4, 2004) *Paleoceanography*, 10.1029/2004PA001028.
46. Curry WB, Oppo DW (March 18, 2005) *Paleoceanography*, 10.1029/2004PA001021.
47. Robinson LF, Adkins JF, Keigwin LD, Southon J, Fernandez DP, Wang S-L, Scheirer DS (2005) *Science* 310:1469–1473.
48. Lynch-Stieglitz J, Adkins JF, Curry WB, Dokken T, Hall IR, Carlos Herguera J, Hirschi JJ-M, Ivanova EV, Kissel C, Marchal O, et al. (2007) *Science* 316:66–69.
49. Venz KA, Hodel DA, Stanton CS, Warnke DA (1999) *Paleoceanography* 14:42–52.
50. Hemming SR (March 18, 2004) *Rev Geophys*, 10.1029/2003RG000128.
51. Denton GH, Broecker WS, Alley RB (2006) *PAGES News* 14:14–16.
52. Oppo DW, Fairbanks RG (1987) *Earth Planet Sci Lett* 86:1–15.
53. Marchitto TM, Curry WB, Oppo DW (1998) *Nature* 393:557–561.
54. Hillaire-Marcel C, de Vernal A, Bilodeau G, Weaver AJ (2001) *Nature* 410:1073–1077.
55. Etter RJ, Grassle JF (1992) *Nature* 360:576–578.
56. Danovaro R, Dell'Anno A, Pusceddu A (2004) *Ecol Lett* 7:821–828.
57. Hunt G, Cronin TM, Roy K (2005) *Ecol Lett* 8:739–747.
58. Rodriguez-Lazaro J, Cronin TM (1999) *Palaeogeogr Palaeoclimatol Palaeoecol* 152:339–364.
59. Gherardi J-M, Labeyrie L, McManus JF, Francois R, Skinner LC, Cortijo E (2005) *Earth Planet Sci Lett* 240:710–723.
60. Keigwin LD, Schlegel MA (June 22, 2002) *Geochem Geophys Geosyst*, 10.1029/2001GC000283.
61. Stirling G, Wilsey B (2001) *Am Nat* 158:286–299.
62. Klován JE, Imbrie J (1971) *Math Geol* 3:61–67.
63. Stuiver M, Reimer PJ (1993) *Radiocarbon* 35:215–230.
64. Stuiver M, Reimer PJ, Reimer RW (2005) CALIB 5.0. Available at: <http://radiocarbon.pa.qub.ac.uk/calib>.
65. Gherardi J-M, Baillie MGL, Bard E, Beck JW, Bertrand CJH, Blackwell PG, Buck CE, Burr GS, Cutler KB, Damon PE, et al. (2004) *Radiocarbon* 46:1059–1086.
66. Druffel ERM (1997) *Science* 275:1454–1457.
67. Hulings NC (1967) *Bull Mar Sci* 17:629–659.
68. Valentine PC (1971) *US Geol Surv Prof Pap* 683D:D1–D28.
69. Cronin TM (1979) *Géogr Phys Quat* 33:121–173.
70. Cronin TM (1990) *US Geol Surv Prof Pap* 1367C:C1–C43.
71. Lyon SK (1990) *US Geol Surv Prof Pap* 1367D:D1–D48.
72. Meeker LD, Mayewski PA (2002) *Holocene* 12:257–266.